Archaeal tetraether membrane lipid fluxes in the northeastern Pacific and the Arabian Sea: Implications for TEX_{86} paleothermometry

Cornelia Wuchter,[1] Stefan Schouten,[1] Stuart G. Wakeham,[2] and Jaap S. Sinninghe Damsté[1]

Received 26 January 2006; revised 3 July 2006; accepted 10 July 2006; published 17 November 2006.

[1] The newly introduced temperature proxy, the tetraether index of archaeal lipids with 86 carbon atoms (TEX_{86}), is based on the number of cyclopentane moieties in the glycerol dialkyl glycerol tetraether (GDGT) lipids of marine Crenarchaeota. The composition of sedimentary GDGTs used for TEX_{86} paleothermometry is thought to reflect sea surface temperature (SST). However, marine Crenarchaeota occur ubiquitously in the world oceans over the entire depth range and not just in surface waters. We analyzed the GDGT distribution in settling particulate organic matter collected in sediment traps from the northeastern Pacific Ocean and the Arabian Sea to investigate the seasonal and spatial distribution of the fluxes of crenarchaeotal GDGTs and the origin of the TEX_{86} signal transported to the sediment. In both settings the TEX_{86} measured at all trap deployment depths reflects SST. In the Arabian Sea, analysis of an annual time series showed that the SST estimate based on TEX_{86} in the shallowest trap at 500 m followed the in situ SST with a 1 to 3 week time delay, likely caused by the relatively low settling speed of sinking particles. This revealed that the GDGT signal that reaches deeper water is derived from the upper water column rather than in situ production of GDGTs. The GDGT temperature signal in deeper traps at 1500 m and 3000 m did not show a seasonal cyclicity observed in the 500 m trap but rather reflected the annual mean SST. This is probably due to a homogenization of the TEX_{86} SST signal carried by particles as they ultimately reach the interior of the ocean. Our data confirm the use of TEX_{86} as a temperature proxy of surface ocean waters.

Citation: Wuchter, C., S. Schouten, S. G. Wakeham, and J. S. Sinninghe Damsté (2006), Archaeal tetraether membrane lipid fluxes in the northeastern Pacific and the Arabian Sea: Implications for TEX_{86} paleothermometry, *Paleoceanography*, *21*, PA4208, doi:10.1029/2006PA001279.

1. Introduction

[2] Recently, a new organic geochemical sea surface temperature proxy, the tetraether index of archaeal lipids with 86 carbon atoms (TEX_{86}) was developed [*Schouten et al.*, 2002]. The TEX_{86} proxy is based on the variations in the number of cyclopentane moieties in the glycerol dibiphytanyl glycerol tetraether (GDGT) membrane lipids of marine Crenarchaeota (see Figure 1 for structures). Marine Crenarchaeota are prokaryotes belonging to the domain of the Archaea that are distributed throughout the world's ocean [*Fuhrman et al.*, 1992; *DeLong*, 1992; *Hoefs et al.*, 1997; *Sinninghe Damsté et al.*, 2002]. It has been estimated that marine Crenarchaeota make up approximately 20% of all picoplankton in marine environments [*Karner et al.*, 2001]. *Schouten et al.* [2002] showed that the relative distributions of marine crenarchaeotal GDGTs with variable numbers of cyclopentane rings in core top sediments from different geographic locations correlate well with sea surface temperature (SST) (Table 1). In cold areas the GDGT lipid containing no cyclopentane moieties (I, Figure 1) and, to a lesser extent, crenarchaeol (V) dominate GDGT distributions. In warmer regions GDGT distributions differ substantially as crenarchaeol is the most abundant GDGT and higher amounts of 1–3 cyclopentane-containing GDGTs (II–IV) and a regio-isomer of crenarchaeol (VI) are also present.

[3] Thermophilic Crenarchaeota, close phylogenetic relatives of the marine Crenarchaeota, vary the number of cyclopentane moieties in the GDGTs of their membrane lipids, an effect that is considered to be a temperature adaptation mechanism of the cell membrane [*Gliozzi et al.*, 1983; *Uda et al.*, 2001]. Recent mesocosm studies have confirmed that Crenarchaeota in North Seawaters have inherited a similar temperature adaptation, presumably from their hyperthermophilic phylogenetic relatives [*Wuchter et al.*, 2004]. With increasing temperature, an increase in the number of cyclopentane moieties was observed. 16S ribosomal DNA analysis revealed that a single crenarchaeotal species was present in the incubated mesocosm tanks leading *Wuchter et al.* [2004] to conclude that the changing GDGT distribution reflects a physiological adaptation to temperature.

[1]Department of Marine Biogeochemistry and Toxicology, Royal Netherlands Institute for Sea Research, Texel, Netherlands.
[2]Skidaway Institute of Oceanography, Savannah, Georgia, USA.

0883-8305/06/2006PA001279$12.00

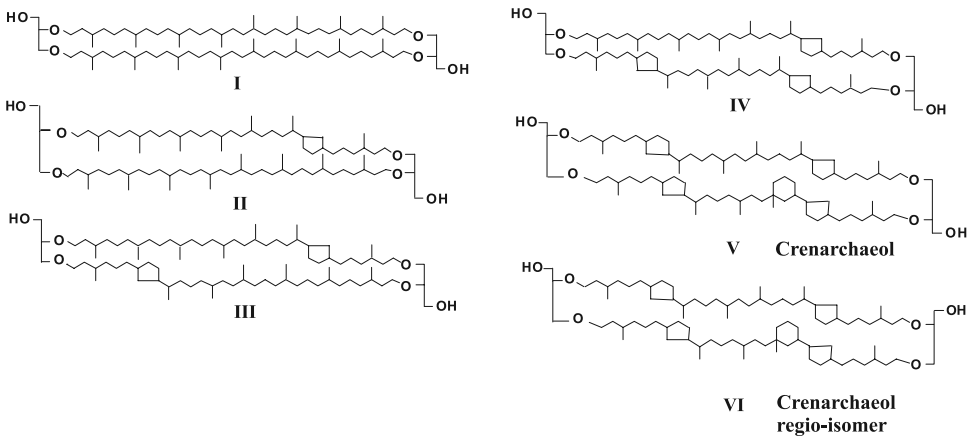

Figure 1. Structures of GDGT membrane lipids of marine pelagic Crenarchaeota.

[4] The observed correlation of TEX_{86} in core top sediments with annual mean SST suggests that the marine crenarchaeotal lipid signal in sediments predominantly reflects GDGTs biosynthesized in the upper part of the water column. This is supported by our study of GDGT distributions in suspended particulate organic matter (POM) from different oceanic regions [*Wuchter et al.*, 2005], which revealed that TEX_{86} correlates well with the upper 100 m water column temperature (Table 1). The TEX_{86} correlation obtained for suspended POM samples was similar to the core top equation although there was more scatter than observed for the core top sediments. The POM samples represented a mixture of fine suspended material, with negligible settling velocities and long residence time in the water column, and more rapidly sinking particles [*Wakeham and Canuel*, 1988] and thus probably contained a mixture of both living and dead crenarchaeotal matter carrying different GDGT distributions.

[5] Our previous studies nonetheless established that the TEX_{86} in suspended POM strongly correlates with SST. However, it had not yet been demonstrated how and when the signal produced in the water column is transported to the sediment floor. For this, the flux of GDGTs and persistence of the TEX_{86} signal through the water column need to be determined. Sediment traps have been used to sample particulate organic matter sinking through the water column and showed the coupling of surface water production with POM flux [*Wakeham and Lee*, 1993]. In the present study, we analyzed the GDGT distributions in settling particulate organic matter using sediment trap collections from the northeastern Pacific Ocean and the Arabian Sea to investigate the seasonal and spatial patterns of the fluxes of crenarchaeotal GDGTs and the TEX_{86} signal.

2. Material and Methods

2.1. Study Sites and Collection of Samples

[6] Sediment trap samples were collected at two stations in the northeastern Pacific during the VERTEX 5 program in 1984 [*Broenkow and Reaves*, 1985; *Silver and Gowing*, 1991]. One station (VERTEX 5A) was located in the centre of the oligotrophic waters of the northeastern Pacific Ocean at 33.3°N, 139.2°W and the other station (VERTEX 5C) was located in the upwelling area near the California coast at 36.1°N, 122.6°W. Free-floating Soutar-type particle interceptor traps (for details see *Wakeham and Canuel* [1988]), with a collecting area of 0.25 m^2, were used to collect sinking, large particles over four different depth intervals (100 m, 250 m, 750 m and 1500 m). Trap deployment periods were 22 days for the oligotrophic setting and 13 days for the upwelling station. $HgCl_2$ was used to inhibit decomposition of the material in the traps. Immediately after recovery of the traps, the collected particulate material was sieved and <300 μm and >300 μm fractions were filtered onto glass fiber filters and frozen at −20°C. The >300 μm fractions consist of large fecal pellets and zooplankton ''swimmers'' [*Lee et al.*, 1988]. The morphology of the VERTEX 5 trap material, both living and detrital, is described in *Michaels et al.* [1990], *Gowing and Coale* [1989], and *Silver and Gowing* [1991].

[7] The Arabian Sea was sampled as part of the US JGOFS program [*Smith et al.*, 1998a]. The site investigated here was located approximately 350 km off the coast of Oman (MS-3: 17°12′N, 59°36′E) at a water depth of

Table 1. Comparison of TEX_{86} Equations Obtained From Core Top Sediments and POM From Different Oceanic Provinces

Origin	Equation	r^2	Number of Samples	Reference
Core tops	$TEX_{86} = 0.015T + 0.29$	0.92	n = 61	*Schouten et al.* [2002]
POM from upper 100 m	$TEX_{86} = 0.017T + 0.29$	0.80	n = 65	*Wuchter et al.* [2005]

3465 m. Three trap arrays at ~500 m, ~1500 m and ~3000 m with varying module configurations (wide mouth traps with 0.37 m^2 collecting areas and narrow mouth traps with 0.018 m^2 collecting areas) and fitted with indented rotating sphere (IRS) valves to minimize collection of swimmers [*Peterson et al.*, 1993] were deployed in November 1994 (R/V *Thomas G. Thomson* cruise TN041), serviced and redeployed in May 1995 (cruise TN047) and recovered after a second time segment in January 1996 (cruise TN050). Carousels in the traps were programmed to collect sinking material over variable time intervals, ranging from 8.5 to 34 days. Shorter intervals were set for monsoon periods when a higher flux was expected. In total for each depth, 22 time-resolved samples were recovered. To inhibit decomposition $HgCl_2$ was used as a biocide [*Lee et al.*, 1992]. Samples were split using a McLane^{TM} WSD-10 wet sample divider, filtered on muffled glass fiber filters, and stored at −20°C until extraction. For more detailed information about the Arabian Sea setting, see *Wakeham et al.* [2002].

2.2. GDGT Analysis

[8] Sediment trap samples were Soxhlet extracted to obtain the lipid extracts used in this study. VERTEX 5 samples (both <300 μm and >300 μm) were extracted with toluene-methanol [*Wakeham and Canuel*, 1988] whereas Arabian Sea filters were extracted with dichloromethane (DCM)-methanol (2:1 by volume [*Wakeham et al.*, 2002]). Lipid extracts were archived in solvent and at −20°C since the time of the original studies until the GDGT analyses made in this study.

[9] An aliquot of the total lipid extract was cleaned on an activated Al_2O_3 column by eluting with methanol/DCM (1:1 by volume). For analysis of GDGTs, the solvent was removed under a stream of nitrogen and the residue was dissolved by sonication (5 min) in hexane/propanol (99:1 by volume). The resulting suspension was filtered through a 0.45 μm pore size, 4 mm diameter Teflon filter prior to analysis. Intact GDGTs were analyzed by high-performance liquid chromatography (HPLC)–atmospheric pressure positive ion chemical ionization mass spectrometry (APCI-MS) by applying conditions slightly modified from *Hopmans et al.* [2000]. Analyses were performed using an HP (Palo Alto, California, USA) 1100 series LC-MS instrument equipped with an autoinjector and Chemstation chromatography manager software. Separation was achieved on a Prevail Cyano column (2.1 × 150 mm, 3 μm; Alltech, Deerfield, Illinois, USA), maintained at 30°C. Injection volumes were 15 μl. GDGTs were first eluted isocratically with 99% hexane and 1% propanol for 5 min, followed by a linear gradient to 1.8% propanol in hexane in 45 min. Flow rate was 0.2 mL/min. After each analysis the column was cleaned by back-flushing hexane/propanol (90:10, by volume) at 0.2 mL/min for 10 min. Detection was achieved using APCI-MS of the eluent. Conditions for APCI-MS were as follows: nebulizer pressure 60 psi, vaporizer temperature 400°C, drying gas (N_2) flow 6 L/min and temperature 200°C, capillary voltage −3 kV, corona 5 μA (~3.2 kV). GDGTs were detected by single ion monitoring of their $[M+H]^+$ ions (dwell time 237 ms) and quantified by integration of the peak areas and a response factor, which was determined by injections of known amounts of a crenarchaeol standard and determination of the resulting peak areas. The analytical error in GDGT abundances is approximately 20%.

[10] For TEX_{86} calculation the peak areas of GDGTs I–VI were integrated and TEX_{86} values were calculated according to the index from *Schouten et al.* [2002] which was defined as follows:

$$TEX_{86} = (III + IV + VI)/(II + III + IV + VI) \quad (1)$$

TEX_{86}-derived SST estimate values were only obtained for samples in which all GDGTs could be detected in sufficient (i.e., 20× background noise) abundance. TEX_{86} temperatures were calculated using the core top correlation (Table 1) obtained by *Schouten et al.* [2002]. Multiple analysis of a batch sediment sample indicated that the reproducibility in TEX_{86} determinations are typically approximately 1°C or better.

3. Results

[11] The crenarchaeotal GDGT flux and distribution at different depths was determined for two VERTEX 5 stations in the northeastern Pacific sampled in June 1984 and over the annual cycle at station MS-3 in the Arabian Sea in 1994–1995.

[12] In the oligotrophic waters in the northeastern Pacific (VERTEX 5A station) GDGT fluxes between 0.2 and 4 μg GDGTs m^{-2} d^{-1} were measured, while those for the station (VERTEX 5C) in the upwelling area were substantially higher (5–97 μg GDGTs m^{-2} d^{-1}) (Figure 2). Generally, a higher GDGT flux was measured below 100 m depth and in the <300 μm trap fractions (Figure 2). The TEX_{86} was 0.56–0.64 for VERTEX 5A in oligotrophic waters and 0.45–0.54 for that at VERTEX 5C in the upwelling area, with no major changes with depth (Table 2). TEX_{86} values of the different size fractions at the same depth showed no substantial difference (Table 2).

[13] The GDGT flux in the time series Arabian Sea trap varied from 0.2 to 35 μg m^{-2} d^{-1} and showed a strong seasonality. At all three trap deployment depths (500, 1500, and 3000 m) the highest flux of GDGTs was measured during the monsoon periods, with the highest flux during the southwest monsoon (SWM) and to a lesser extent during the northeast monsoon (NEM) (Figure 3a). During the summer intermonsoon (SI) and fall intermonsoon (FI) the flux was generally low. In the trap deployed at 1500 m the GDGT flux was generally twice as high as in the 500 m trap during monsoon times, whereas those at 3000 m was substantially lower than at 500 m. The TEX_{86} varied between 0.66 and 0.75 (Table 3). At 500 m depth, a pronounced seasonal variation in the TEX_{86} signal is observed, but seasonal variations were less pronounced at 1500 and 3000 m (Figure 4).

4. Discussion

4.1. Variation in GDGT Flux With Depth in the Water Column

[14] In both of the oceanic regimes we studied, the GDGT flux increased below 100 m depth. Maximum GDGT flux

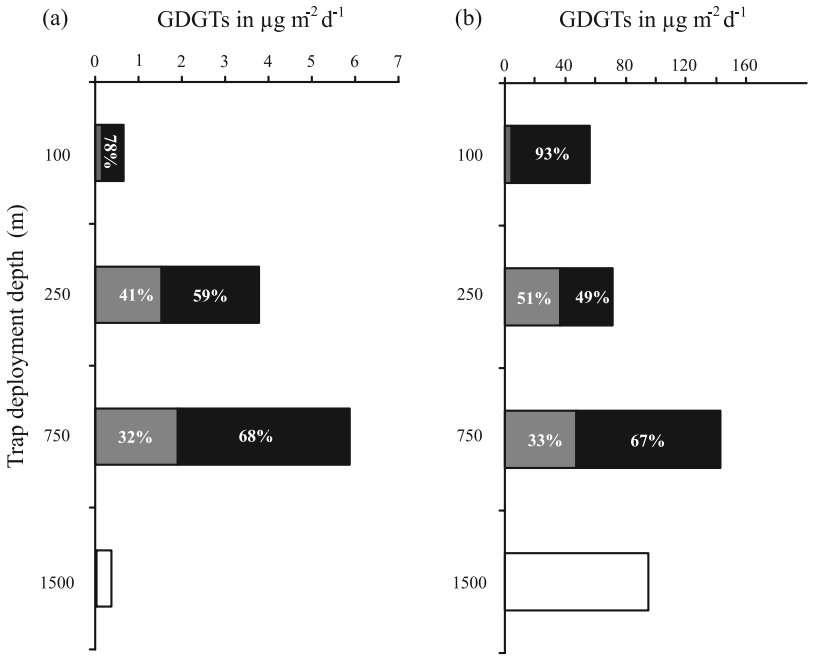

Figure 2. The GDGT flux at different depths and in different size classes at VERTEX 5 stations in the northeastern Pacific Ocean. Traps were deployed (a) in an oligotrophic setting (VERTEX 5A) and (b) at an upwelling site near the California Coast (VERTEX 5C). Shaded bars represent the size fraction >300μm, and solid bars represent size fraction <300 μm. Numbers in bars represent the percentage of the different size fractions of the total GDGT flux. Open bars represent samples at 1500 m for which size fractions were combined.

was measured at 750 m in the oligotrophic waters of VERTEX 5A and in the upwelling area of VERTEX 5C (Figure 2), and in the Arabian Sea the GDGT flux was highest in the mid water trap at 1500 m (Figure 3). Whereas the Arabian Sea traps used the indented rotating sphere (IRS) valve and thus contained few zooplankton swimmers [*Wakeham et al.*, 2002], the VERTEX 5 study was undertaken before the IRS valve was developed and therefore the traps contained a large number of large swimmers, including crustaceans, pteropods, and radiolarians in the >300 μm size fraction (S. G. Wakeham, shipboard observations, 1984; *Michaels et al.*, 1990; *Gowing and Coale*, 1989; *Silver and Gowing*, 1991].

[15] Although particle fluxes are frequently highest in the epipelagic zone and decrease with depth, deep water flux maxima for sinking particulate and associated inorganic and organic constituents are not uncommon [see *Wakeham and Lee*, 1993, and references therein; *Wakeham et al.*, 2002, and references therein]. Several processes have been invoked to explain this observation. GDGT production is

Table 2. TEX_{86} Values and Calculated TEX_{86} Temperature Compared to Annual Mean SST at the Two Sampling Sites at the Northeastern Pacific Ocean[a]

	TEX_{86}		TEX_{86} Temperature, °C			
Depth, m	>300 μm	<300 μm	>300 μm	<300 μm	Mean in Situ T, °C	Annual Mean SST, °C
			VERTEX 5A			
100	ND	ND	ND	ND	18	
250	0.64	0.60	23.3	20.7	10	
750	0.57	0.56	18.7	18.0	4.5	
1500[b]	ND		ND		2.8	
Average[c]	0.61 ± 0.05	0.58 ± 0.03	21.0 ± 3.3	19.4 ± 1.9		20
			VERTEX 5C			
100	0.51	0.52	14.7	15.3	9	
250	0.54	0.49	16.7	13.3	7	
750	0.45	0.46	10.7	11.3	4.5	
1500[a]	0.52		15.3		2.8	
Average[c]	0.50 ± 0.05	0.50 ± 0.03	14.0 ± 3.1	13.8 ± 1.9		14

[a]ND is not determined.
[b]Two size fractions were combined.
[c]Standard deviations are also provided.

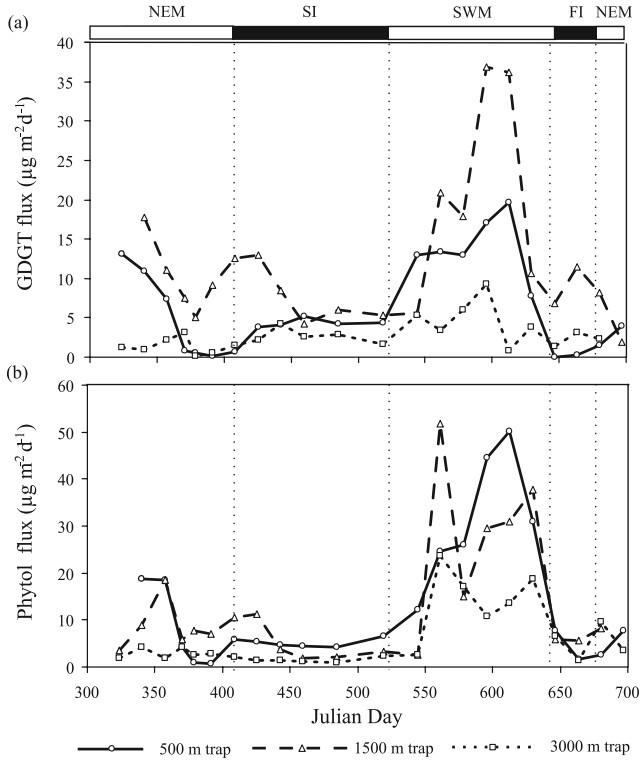

Figure 3. (a) GDGT and (b) phytol fluxes for the indented rotating spheres C traps at MS-3 in the Arabian Sea. The phytol fluxes were determined previously [*Wakeham et al.*, 2002] and are reported at http://usjgofs.whoi.edu/jg/dir/jgofs/arabian/. Bars at the top of the plot and dotted vertical lines indicate the monsoon periods based on *Weller et al.* [1998]. Abbreviations are NEM, northeast monsoon; SI, spring intermonsoon; SWM, southwest monsoon; and FI, fall intermonsoon. Data points represent the center of collection intervals. Solid lines represent the shallow trap at ~500 m, the dashed lines correspond to the mid trap at ~1500 m, and the stippled lines represent the deep trap at ~3000 m depth.

generally assumed to occur primarily in surface waters, but concentrations of GDGTs in suspended particles at both the VERTEX 5 and Arabian Sea sites are also elevated at mid depth [*Sinninghe Damsté et al.*, 2002; *Wuchter et al.*, 2005] suggesting mid water production as well. Passively sinking particles containing surface-derived GDGTs that might accumulate at density discontinuities within the water column have been suggested as causing mid water flux maxima [*Karl et al.*, 1976]. Migrating zooplankton that feed in surface waters but migrate and defecate at depth [*Urrère and Knauer*, 1981; *Karl and Knauer*, 1984; *Wishner et al.*, 1998] would provide an active transport mechanism whereby organic matter could bypass a shallower trap yet be collected in a deeper one. In the northeast Pacific at both VERTEX sites an increase in the ratio of GDGTs derived from the larger (>300 μm) size fraction was observed in water below 100 m depth (Figure 2). We believe that the GDGTs in the larger size fraction are derived from Crenarchaeota in surface waters but are carried to depth by migrating zooplankton. In the Arabian Sea, where a swimmer contribution was minimal to the trap "flux," vertical migration of zooplankton, including into the oxygen minimum zone [*Smith et al.*, 1998b; *Wishner et al.*, 1998], is a likely active biological transport mechanism for bypassing the trap at 500 m depth and carrying GDGTs directly to 1500 m.

[16] Horizontal advective processes such as lateral transport probably also play an important role in transporting material into the interior of the ocean. Lateral advection of sedimentary material from the California Margin into the northeastern Pacific has been observed [*Karl and Knauer*, 1984] and has been invoked as resulting in mid water flux maxima [*Silver and Gowing*, 1991], possibly including the GDGT flux maximum we observe. The monsoon-driven physical processes in the Arabian Sea are well known for producing eddies and filaments that move water, nutrients, plankton, resuspended continental margin sediments and water column particulate matter offshore [*Smith et al.*, 1998a and references therein]. Lateral transport of suspended sediments off the Arabian shelf is thought to be an important influence in water column particle fluxes [*Witte and Pfannkuche*, 2000]. Especially in highly physically dynamic areas such as the Arabian Sea, sediment traps are considered to collect material sinking through a cone of the water column [*Siegel and Deuser*, 1997]. Particles sinking with oblique trajectories might well originate "up current" from the sediment trap location, and in the Arabian Sea this decoupling of surface water processes and deep-water collections is likely [*Honjo et al.*, 1999; *Wakeham et al.*, 2002]. In the Arabian Sea the particle catchment area might be as large as 10^3–10^4 km^2 [*van Gyldenfeldt et al.*, 2000], resulting in a marked homogenization of organic matter compositions by the time particles are collected in deep traps.

4.2. Seasonal Variation in the GDGT Flux in the Arabian Sea

[17] The time series record in the Arabian Sea shows that at all three deployment depths the highest GDGT flux occurred during the SWM (Figure 3a). This is consistent with previous studies showing that the maximum flux of organic matter and biomarker lipids occurred during the SWM, regardless of trap deployment depth and location [*Wakeham et al.*, 2002]. The highest GDGT flux occurred at the same time as the highest flux of phytol (Figure 3b), where phytol is a general biomarker for photoautotrophic plankton as it is derived from chlorophyll. This GDGT flux pattern is not entirely consistent with the conclusions regarding the ecology of marine Crenarchaeota which suggest them to be chemolithoautotrophs [*Wuchter et al.*, 2003; *Herndl et al.*, 2005; *Könneke et al.*, 2005; *Wuchter et al.*, 2006]. As chemolithoautotrophs, Crenarchaeota in surface waters would compete with phytoplankton for nutrients (e.g., ammonium), and crenarchaeotal abundance is often negatively correlated with that of phytoplankton as reported for different oceanic regimes [*Murray et al.*, 1998, 1999; *Massana et al.*, 1997; *Wuchter*, 2006]. One might therefore expect lower cell numbers in the Arabian Sea for Crenarchaeota during periods of high phytoplankton productivity

Table 3. TEX_{86} Values, TEX_{86} Temperature, and Flux Weighted Mean TEX_{86} Temperature at the Three Trap Deployment Depths Compared to in Situ Annual Mean SST at the MS-3 Station in the Arabian Sea

		500 m Trap		1500 m Trap		3000 m Trap	
	In Situ SST, °C[a]	TEX_{86}	TEX_{86} T, °C	TEX_{86}	TEX_{86} T, °C	TEX_{86}	TEX_{86} T, °C
Julian Day							
315–332	27.0	0.73	29.3	0.69	26.6	0.67	25.6
332–349	26.0	0.71	27.8	0.71	28.1	0.67	25.6
349–366	25.1	0.70	27.3	0.71	28.2	0.68	26.0
366–375	24.9	0.69	26.5	0.71	27.8	0.68	26.0
375–383	24.5	0.69	26.6	0.69	26.7	0.68	25.8
383–400	24.8	0.68	26.2	0.71	27.7	ND	ND
400–417	24.5	0.69	26.5	0.69	26.9	0.67	25.6
417–434	24.9	0.69	26.8	0.70	27.2	0.67	25.1
434–451	25.6	0.70	27.6	0.71	28.0	0.66	24.9
451–468	26.8	0.71	28.0	0.72	28.4	0.69	26.7
468–502	28.3	0.71	28.1	0.72	28.8	0.70	27.3
502–536	28.8	0.74	29.8	0.72	28.8	0.71	27.9
536–553	27.1	0.75	30.6	0.72	28.6	0.68	26.0
553–570	25.9	0.74	29.9	0.71	27.8	0.69	26.8
570–587	25.1	0.73	29.4	0.74	29.8	0.70	27.0
587–604	24.6	0.67	25.5	0.71	28.0	0.69	26.8
604–621	25.0	0.67	25.3	0.70	27.6	0.70	27.1
621–638	26.3	0.67	25.6	0.71	28.2	ND	ND
638–655	27.5	ND	ND	0.72	28.8	0.70	27.3
655–672	27.8	0.70	27.6	0.71	28.1	0.69	27.0
672–689	27.1	0.70	27.2	0.66	24.9	0.69	26.9
689–705	26.4	0.70	27.6	0.68	26.2	0.67	25.1
In situ annual mean, °C	26.4						
Standard deviation		0.02	1.5	0.02	1.1	0.01	0.8
Flux weighted mean		0.71	27.8	0.71	27.9	0.69	26.6

[a]The average in situ SST for each trap deployment time interval was calculated from satellite data of the Pathfinder advanced very high resolution radiometer (AVHRR) data set at http:podaac.jpl.nasa.gov.

(i.e., the SWM). Yet we observe similar flux patterns for phytol and GDGTs (Figure 3).

[18] However, the higher flux of GDGTs during the SWM needs not a priori imply a higher abundance of Crenarchaeota during the SWM but could also result if crenarchaeotal cells were at that time more efficiently transported to depth by packaging of crenarchaeotal cells by grazing zooplankton. In fact, this is likely the most important transport mechanism for GDGTs as crenarchaeotal cells are too small (< 1 μm) and not sufficiently dense to sink as individual cells [*Wakeham et al.*, 2003]. Indeed, the *relative* increase in the GDGT flux between SI and SWM at 500 m is substantially smaller than that of biomarker lipids derived from photoautotrophic organisms (i.e., diatoms and haptophytes), and even of total particles and organic carbon (Table 4). High mass and organic matter fluxes during the SWM are caused by enhanced photoautotrophic production in response to upwelling of nutrients near the coast of Oman. In turn, high primary production leads to a highly active food web in the upper water column, with phytodetritus settling into deeper waters as marine snow or zooplankton fecal matter [*Wakeham and Canuel*, 1988; *Wakeham et al.*, 2002]. Thus we suggest that the high flux of GDGTs during the SWM is caused by a more efficient food web-based scavenging of archaeal cells, probably attached to aggregates or in fecal pellets, and not necessarily by higher crenarchaeotal cell abundances.

4.3. TEX_{86} and Size Fraction

[19] Sediment trap material at the VERTEX 5 sites was sieved to remove large swimmers in order to better determine the composition of passively sinking material. Remarkably, there was little difference in TEX_{86} between the two size classes (Table 2), even though there was a substantial ''flux'' by swimmers (Figure 2). Our data suggest that alteration of GDGTs caused by grazing and digesting by zooplankton does not substantially change the GDGT distribution and that the signal from surface waters remains intact for both passively sinking and actively transported material.

4.4. Variations in TEX_{86} With Depth

[20] Marine Crenarchaeota occur over a large depth range in the ocean [*Karner et al.*, 2001; *Herndl et al.*, 2005], accounting for roughly half of the prokaryotes in the bathypelagic ocean, and are thus exposed to a wide range of ambient temperatures, down to ~5°C in the bathypelagic zone. GDGT concentrations in suspended particulate matter are most abundant in the mesopelagic zones of both the VERTEX 5 sites (at 750 m [*Wuchter et al.*, 2005]) and the Arabian Sea sites (at 500 m [*Sinninghe Damsté et al.*, 2002]), yet TEX_{86} values do not reflect the <12°C ambient temperatures. Likewise, the TEX_{86} values in sediment trap-collected material was remarkably constant throughout the water column (Table 2) in both the Pacific and Arabian Sea, in spite of substantial seasonal and depth-related variations in GDGT flux and decreasing water temperatures with increasing depth. Thus, at neither site did the calculated TEX_{86} temperatures reflect in situ temperature at the different trap deployment depths, but rather correlated best with the annual mean SST (Table 2). Coupling the sea surface GDGT production and its SST signal to the sedi-

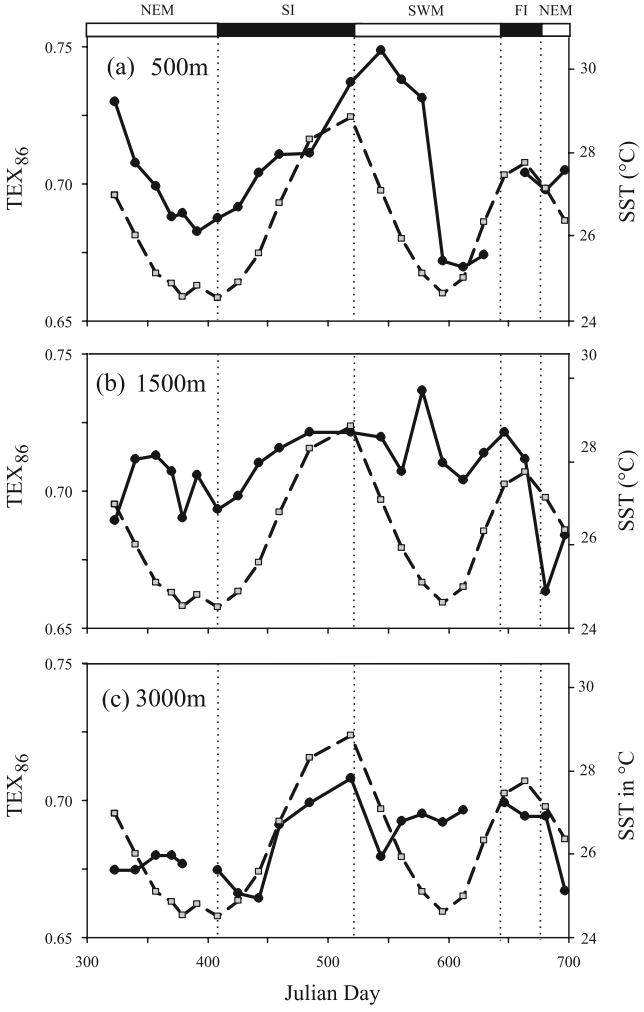

Figure 4. Seasonal variations in in situ SSTs (dashed lines) and calculated TEX_{86} SSTs (solid lines) using the core top calibration of *Schouten et al.* [2002] in traps deployed at (a) 500, (b) 1500, and (c) 3000 m depth at MS-3 station in the Arabian Sea. The solid lines also refer to measured TEX_{86} values (left scale). Missing data points represent samples with insufficient amounts of GDGTs for TEX_{86} calculation. In situ SSTs were obtained from the Pathfinder advanced very high resolution radiometer data set at http:podaac.jpl.nasa.gov and were averaged over the trap deployment periods.

ment, the primary assumption of the TEX_{86} proxy, requires that GDGTs from the surface are more efficiently transported downward, whereas GDGTs produced in colder waters at depth are not. The similar TEX_{86} values from the sinking particle fractions down the water column show that the sinking GDGTs are mostly derived from the upper part of the ocean and that the GDGTs derived from Crenarchaeota living in deeper water do not contribute substantially to the GDGT flux and thus the TEX_{86} signal reaching the sediment. This conclusion is consistent with the previous results of *Wuchter et al.* [2005] on GDGTs showing a strong correlation between TEX_{86} values of suspended POM from depth profiles in different oceanic regimes with SST rather than in situ temperature [*Wuchter et al.*, 2005]. In addition, a study of GDGTs in suspended POM and sediment traps from the Black Sea [*Wakeham et al.*, 2003] showed that high amounts of ^{13}C-depleted GDGTs in suspended POM in the deep anoxic zone could not be found in sediment traps and the underlying sediments. The authors suggested that because of the absence of grazing in the anoxic zone of the Black Sea, GDGTs biosynthesized in deep waters lack a packaging mechanism that allows transport to the seafloor, and thus the dominant GDGT flux occurs from the upper water column were an active food web exists to package GDGTs into sinking particles [*Wakeham et al.*, 2003].

4.5. Seasonal Variation in TEX_{86} in the Arabian Sea

[21] The TEX_{86} measured at the shallow 500 m trap in the Arabian Sea showed a pronounced seasonal trend which followed that of the in situ SST obtained by satellite observations (Figure 4a), with an apparent lag of 1–3 weeks. The time a particle needs to sink and be captured in the 500 m trap likely causes this time offset in the TEX_{86} signal. Fine particles move through the water column at rates of a few meters per day [*Krishnaswami et al.*, 1981; *Bacon and Anderson*, 1982], whereas fecal pellets and marine snow may sink at rates of tens to hundreds of m d^{-1} [e.g., *Small et al.*, 1979; *McCave*, 1984; *Asper*, 1987]. The signal that reaches the trap at 500 m is an integrated signal of particles of different size classes and sinking speed. The offset of 1–3 weeks in the 500 m trap indicates that the captured particles sink through the water column on average at 25–75 m d^{-1}, and this is well in the range with the above mentioned particle sinking speeds. While the 500 m trap shows a seasonal cycling in TEX_{86}, the mid water trap at 1500 m and the deep trap at 3000 m do not show a

Table 4. Average Fluxes of Total Particles, Organic Carbon, and Different Biomarkers During Spring Intermonsoon and Southwest Monsoon at the 500 m trap at MS-3 Station in the Arabian Sea[a]

		Average Flux, μg m^{-2} d^{-1}		
Fraction/Biomarker	Origin	Spring Intermonsoon	Southwest Monsoon	Relative Increase, %
Total particles		60×10^3	360×10^3	600
Organic carbon		6×10^3	28×10^3	470
Phytol	phototrophs	5	28	560
$C_{25:3}$ HBI	Rhisozolenoid diatoms	0.3	17	5700
C_{30} alkane-1,14-diol	Proboscia diatoms	3	25	830
$C_{37:2}$ alkenones	Haptophytes	0.4	5	1300
GDGTs	marine Crenarchaeota	4	12	300

[a]Flux data are from *Wakeham et al.* [2002] except for the GDGTs (this study).

corresponding seasonality in TEX_{86} (Figures 4b and 4c). A similar phenomenon was observed for SST reconstructed from alkenones in a trap at 2200 m depth in the Arabian Sea [*Prahl et al.*, 2000] and for other lipids in deep Arabian Sea traps [*Wakeham et al.*, 2002]. The mid water and deep traps are also likely to collect material that carries an integrated GDGT signal derived from a larger area, including influences of lateral transport of material produced up current. In spite of a slight offset between SSTs obtained by satellite and TEX_{86} measurements, the trap at 500 m shows for the first time that the TEX_{86} tracks the seasonal SST cycle, demonstrating that this proxy captures upper water column temperatures. The TEX_{86} SST signal measured at 500 m is on average approximately 1°C higher than the SST measured in situ. This temperature offset could be due to the fact the calibration equation used is derived from core tops from many oceanic areas [*Schouten et al.*, 2002] and this calibration differs slightly from a suspended POM-derived calibration [*Wuchter et al.*, 2005]. The core top calibration line slightly overestimates SSTs at high temperatures such as those in the Arabian Sea, whereas if the equation derived from POM (Table 1) was used the SST estimates would be ~1.5°C lower than in situ SST. Further development of the TEX_{86} SST calibration is required to see if there is a systematic offset between suspended POM, sediment traps and core tops or whether the calibration can be improved further.

[22] Nonetheless, the calculated flux-weighted mean TEX_{86} SST in the three traps of the Arabian Sea deployed at different depths do indeed reflect annual mean SST (Table 3). The calculated flux-weighted mean TEX_{86} SSTs for the 500 m and the 1500 m trap are approximately 1°C higher than for the 3000 m trap (Table 3). The calculated annual mean in situ SST during the trap deployment period is nearly the same as the calculated flux-weighted mean TEX_{86} SST signal from the 3000 m trap (Table 3). This shows that even if in the upper parts of the water column the TEX_{86} in descending particles reflects seasonal variations in SST, the GDGT signal that reaches the deep water and sediment reflects an integrated signal and the corresponding TEX_{86} reflects annual mean SST. Thus the SST-TEX_{86} signal carried through the water column appears to be robust, at least in the Arabian Sea, despite potential complications due to lateral transport and mixing mechanisms of organic matter, and our results help to explain why TEX_{86} in core top sediments from different geographic locations correlates well with annual mean SST.

5. Conclusions

[23] Our data show that the TEX_{86} signal in GDGTs contained in sinking particles in the water column of the northeastern Pacific and Arabian Sea reflects SST and confirms that the GDGT signal which reaches the sediment is mainly produced in the upper water layer. There is no evidence that mesopelagic or bathypelagic Crenarchaeota living at lower temperatures than SST substantially contribute to the TEX_{86} signal. The TEX_{86} is relatively invariant in different size fractions throughout the water column, suggesting that alteration due to grazing, repackaging and active transport of surface-derived GDGTs by zooplankton does not appear to substantially influence the GDGT distribution and thus the TEX_{86}. In the Arabian Sea time series we observed a strong correlation of the TEX_{86} in the upper 500 m trap with seasonal SST. The TEX_{86} signal which reaches deep traps during the annual cycle did not show the corresponding seasonality but rather reflected annual mean SST. This deep water temperature signal is probably strongly influenced by a homogenization of particles derived from a large production area in surface waters and therefore the TEX_{86} in deeper waters or in sediment rather reflects an integrated annual mean SST from which any seasonal SST signal has been lost. Data presented here strengthen the potential for using the TEX_{86} for reconstruction of upper water column temperatures in ancient environments from sedimentary records of TEX_{86}.

[24] **Acknowledgments.** We thank Martijn Woltering (NIOZ) for assistance in sample processing and Ellen Hopmans (NIOZ) for assistance and advice on the HPLC/MS analyses. Thanks also go to numerous personnel who helped in sample collection during VERTEX and JGOFS cruises. The U.S. National Science Foundation supported the Arabian Sea cruise, and the U.S. Office of Naval Research supported sample collection on VERTEX.

References

Asper, V. L. (1987), Measuring the flux and sinking speed of marine snow aggregates, *Deep Sea Res., Part A*, *34*, 1–17.

Bacon, M. P., and R. F. Anderson (1982), Distribution of thorium isotopes between dissolved and particulate forms in the deep sea, *J. Geophys. Res.*, *87*, 2045–2056.

Broenkow, W. W., and R. E. Reaves (1985), Oceanographic results from the Vertex 5 particle trap experiment across the California current May–July 1984, *Tech. Publ. 85–2*, 110 pp., Moss Landing Mar. Lab., Moss Landing, Calif.

DeLong, E. F. (1992), Archaea in coastal marine environments, *Proc. Natl. Acad. Sci. U. S. A.*, *89*, 5685–5689.

Fuhrman, J. A., K. McCallum, and A. A. Davis (1992), Novel major archaebacterial group from marine plankton, *Nature*, *356*, 148–149.

Gliozzi, A., G. Paoli, M. De Rosa, and A. Gambacorta (1983), Effect of isoprenoid cyclization on the transition temperature of lipids in thermophilic archaebacteria, *Biochim. Biophys. Acta*, *735*, 234–242.

Gowing, M. M., and S. L. Coale (1989), Fluxes of living radiolarians and their skeletons along a northeast Pacific transect from coastal upwelling to open ocean waters, *Deep Sea Res., Part A*, *36*, 561–576.

Hoefs, M. J. L., S. Schouten, J. W. de Leeuw, L. L. King, S. G. Wakeham, and J. S. Sinninghe Damsté (1997), Ether lipids of planktonic Archaea in the marine water column, *Appl. Environ. Microbiol.*, *63*, 3090–3095.

Herndl, G. J., T. Reinthaler, E. Teira, H. van Aken, C. Veth, A. Pernthaler, and J. Pernthaler (2005), Contribution of Archaea to total prokaryotic production in the deep Atlantic Ocean, *Appl. Environ. Microbiol.*, *71*, 2303–2309.

Honjo, S., J. Dymond, W. Prell, and V. Ittekkot (1999), Monsoon-controlled export fluxes to the interior of the Arabian Sea, *Deep Sea Res., Part II*, *46*, 1859–1902.

Hopmans, E. C., S. Schouten, R. D. Pancost, M. T. J. Van der Meer, and J. S. Sinninghe Damsté (2000), Analysis of intact tetraether lipids in archaeal cell material and sediments by high performance liquid chromatography/atmospheric pressure chemical ionization mass spectrometry, *Rapid Commun. Mass Spectrom.*, *14*, 585–589.

Karl, D. M., and G. A. Knauer (1984), Vertical distribution, transport and exchange of carbon in the northeast Pacific Ocean: Evidence for multiple zones of biological activity, *Deep Sea Res., Part A*, *31*, 221–243.

Karl, D. M., P. A. LaRock, J. W. Morse, and W. Sturges (1976), Adenosin triphosphate in the North Atlantic Ocean and its relationship to the oxygen minimum, *Deep Sea Res. Oceanogr. Abstr.*, *23*, 81–88.

Karner, M. B., E. F. DeLong, and D. M. Karl (2001), Archaeal dominance in the mesopelagic zone of the Pacific Ocean, *Nature*, *409*, 507–510.

Könneke, M., A. E. Bernhard, J. R. de la Torre, C. B. Walker, J. B. Waterbury, and D. A. Stahl (2005), Isolation of an autotrophic ammonia-oxidizing marine archaeon, *Nature*, *437*, 543–546.

Krishnaswami, S., M. M. Sarin, and B. L. K. Somayajulu (1981), Chemical and radiochemical investigations of surface and deep particles of the Indian Ocean, *Earth Planet. Sci. Lett.*, *54*, 81–96.

Lee, C., S. G. Wakeham, and J. I. Hedges (1988), The measurement of oceanic particle flux—Are "swimmers" a problem?, *Oceanography*, *1*, 34–36.

Lee, C., J. I. Hedges, S. G. Wakeham, and N. Zhu (1992), Effectiveness of poisons and preservatives in retarding bacterial activity in sediment trap material, *Limnol. Oceanogr.*, *37*, 117–130.

Massana, R., A. E. Murray, C. M. Preston, and E. F. DeLong (1997), Vertical distribution and phylogenetic characterization of marine planktonic Archaea in the Santa Barbara Channel, *Appl. Environ. Microbiol.*, *63*, 50–56.

McCave, I. N. (1984), Size spectra and aggregation of suspended particles in the deep ocean, *Deep Sea Res., Part A*, *31*, 329–352.

Michaels, A. F., M. W. Silver, M. M. Gowing, and G. A. Knauer (1990), Cryptic zooplankton: "Swimmers" in upper ocean sediments traps, *Deep Sea Res., Part A*, *37*, 1285–1296.

Murray, A. E., C. M. Preston, R. Massana, L. T. Taylor, A. Blakis, K. Wu, and E. F. DeLong (1998), Seasonal and spatial variability of bacterial and archaeal assemblages in the coastal waters near Anvers Island, Antarctica, *Appl. Environ. Microbiol.*, *64*, 2585–2595.

Murray, A. E., A. Blankis, R. Massana, S. Strawzewski, U. Passow, A. Alldredge, and E. F. DeLong (1999), A time series assessment of planktonic archaeal variability in the Santa Barbara Channel, *Aquat. Microb. Ecol.*, *20*, 129–145.

Peterson, M. L., P. J. Hernes, D. J. Thoreson, J. I. Hedges, C. Lee, and S. G. Wakeham (1993), Field evaluation of a valved sediment trap, *Limnol. Oceanogr.*, *38*, 1741–1761.

Prahl, F. G., J. Dymond, and M. A. Sparrow (2000), Annual biomarker record for export production in the central Arabian Sea, *Deep Sea Res., Part II*, *47*, 1581–1604.

Schouten, S., E. C. Hopmans, E. Schefuss, and J. S. Sinninghe Damsté (2002), Distributional variations in marine crenarchaeotal membrane lipids: A new tool for reconstructing ancient sea water temperatures?, *Earth. Planet. Sci Lett.*, *204*, 265–274.

Siegel, D. A., and W. G. Deuser (1997), Deep ocean time-series particle trapping in the Sargasso Sea: The modelling of "statistical funnels", *Deep Sea Res., Part I*, *44*, 1519–1541.

Silver, M. W., and M. M. Gowing (1991), The "particle" flux: Origins and biological components, *Prog. Oceanogr.*, *26*, 75–113.

Sinninghe Damsté, J. S., W. I. C. Rijpstra, E. C. Hopmans, F. Prahl, S. G. Wakeham, and S. Schouten (2002), Distribution of membrane lipids of planktonic Crenarchaeota in the Arabian Sea, *Appl. Environ. Microbiol.*, *68*, 2997–3002.

Small, L. F., S. W. Fowler, and M. Y. Ünlü (1979), Sinking rates of natural copepod fecal pellets, *Mar. Biol.*, *51*, 233–241.

Smith, S. L., L. A. Codispoti, J. M. Morrison, and R. T. Barber (1998a), The 1994–1996 Arabian Sea Expedition: An integrated, interdisciplinary investigation of the response of the northwestern Indian Ocean to monsoonal forcing, *Deep Sea Res., Part II*, *45*, 1905–1915.

Smith, S., M. Roman, I. Prusova, K. Wishner, K. Gowing, L. A. Codispoti, R. Barber, J. Marra, and C. Flagg (1998b), Seasonal response of zooplankton to monsoonal reversals in the Arabian Sea, *Deep Sea Res., Part II*, *45*, 2369–2403.

Uda, I., A. Sugai, Y. H. Itoh, and T. Itoh (2001), Variation in molecular species of polar lipids from *Thermoplasma acidophilum* depends on growth temperature, *Lipids*, *36*, 103–105.

Urrère, M. A., and G. A. Knauer (1981), Zooplankton fecal pellet fluxes and vertical transport of particulate organic material in the pelagic environment, *J. Plankton Res.*, *3*, 369–387.

van Gyldenfeldt, A. B., J. Carstens, and J. Meincke (2000), Estimation of catchment area of sediment trap by means of current meters and foraminiferal tests, *Deep Sea Res., Part II*, *47*, 1701–1717.

Wakeham, S. G., and E. A. Canuel (1988), Organic geochemistry of particulate matter in the eastern tropical North Pacific Ocean: Implications for particle dynamics, *J. Mar. Res.*, *46*, 183–213.

Wakeham, S. G., and C. Lee (1993), Production, transport, and alteration of particulate organic matter in the marine water column, in *Organic Geochemistry*, edited by M. H. Engel and S. A. Macko, pp. 145–169, Springer, New York.

Wakeham, S. G., M. L. Peterson, J. I. Hedges, and C. Lee (2002), Lipid biomarker fluxes in the Arabian Sea, with a comparison to the equatorial Pacific Ocean, *Deep Sea Res., Part II*, *49*, 2265–2301.

Wakeham, S. G., C. M. Lewis, E. C. Hopmans, S. Schouten, and J. S. Sinninghe Damsté (2003), Archaea mediate anaerobic oxidation of methane in deep euxinic waters of the Black Sea, *Geochim. Cosmochim. Acta*, *67*, 1359–1374.

Weller, R. A., M. M. Baumgartner, S. A. Josey, A. S. Fischer, and J. C. Kindler (1998), Atmospheric forcing in the Arabian Sea during 1994–1995: Observations and comparisons with climatology and models, *Deep Sea Res., Part II*, *45*, 1961–1999.

Wishner, K. F., M. M. Gowing, and C. Gelfman (1998), Mesozooplankton biomass in the upper 1000 m in the Arabian Sea: Overall seasonal and geographic patterns, and relationship to oxygen gradients, *Deep Sea Res., Part II*, *45*, 2405–2431.

Witte, U., and O. Pfannkuche (2000), High rates of benthic carbon remineralization in the abyssal Arabian Sea, *Deep Sea Res., Part II*, *47*, 2785–2804.

Wuchter, C. (2006), Ecology and membrane lipid distribution of marine Crenarchaeota: Implications for TEX_{86} paleothermometry, *Geol. Ultraiectina*, *257*, 147 pp.

Wuchter, C., S. Schouten, H. T. S. Boschker, and J. S. Sinninghe Damsté (2003), Bicarbonate uptake by marine Crenarchaeota, *FEMS Microbiol. Lett.*, *219*, 203–207.

Wuchter, C., S. Schouten, M. J. L. Coolen, and J. S. Sinninghe Damsté (2004), Temperature-dependent variation in the distribution of tetraether membrane lipids of marine Crenarchaeota: Implications for TEX_{86} paleothermometry, *Paleoceanography*, *19*, PA4028, doi:10.1029/2004PA001041.

Wuchter, C., S. Schouten, S. G. Wakeham, and J. S. Sinninghe Damsté (2005), Temporal and spatial variation in tetraether membrane lipids of marine Crenarchaeota in particulate organic matter: Implications for TEX_{86} paleothermometry, *Paleoceanography*, *20*, PA3013, doi:10.1029/2004PA001110.

Wuchter, C., L. Herfort, M. J. L. Coolen, B. Abbas, P. Timmers, M. Strous, G. J. Herndl, J. J. Middelburg, S. Schouten, and J. S. Sinninghe Damsté (2006), Archaeal nitrification in the ocean, *Proc. Natl. Acad. Sci. U. S. A.*, *103*, 12,317–12,322.

S. Schouten, J. S. Sinninghe Damsté, and C. Wuchter, Department of Marine Biogeochemistry and Toxicology, Royal Netherlands Institute for Sea Research, P.O. Box 59, 1790AB Den Burg, Texel, Netherlands. (damste@nioz.nl)

S. G. Wakeham, Skidaway Institute of Oceanography, 10 Ocean Science Circle, Savannah, GA 31411, USA.